Journal of Glycomics & Lipidomics

Research Article   **Open Access**

Metabolic Profiling and Quantification of Sphingolipids by Liquid Chromatography-Tandem Mass Spectrometry

Wujuan Zhang[1], Brian Quinn[2], Sonya Barnes[2], Gregory A Grabowski[2,3], Ying Sun[2,3] and Kenneth Setchell[1*,3]

[1]TheDepartment of Pathology and Laboratory Medicine, Cincinnati Children's Hospital Medical Center, Cincinnati, Ohio, USA
[2]TheDivision of Human Genetics, Cincinnati Children's Hospital Medical Center, Cincinnati, Ohio, USA
[3]The Department of Pediatrics, University of Cincinnati College of Medicine, Cincinnati, Ohio, USA

Abstract

A precise, robust, and specific liquid chromatography-electrospray tandem mass spectrometry (LC-ESI-MS/MS) method was developed for profiling and quantifying glucosyl sphingosine (GS), glucosylceramide (GC), ceramide (Cer), lactosylceramide (LacCer) and sulfatide lipid species in a variety of mouse tissues. The linear response ranges of these species were 0.05-25 ng. The major GC species identified in visceral tissues of mice were GCs with N-acyl chains of C24-1, C24, C22, C16 lengths, but the qualitative and quantitative profiles differed among tissues. GC levels in spleen were approximately 3-5 times higher than in liver and lung. Brain differed from visceral tissues in that galactosylceramides (GalCer) were the predominant monohexosylceramide species identified. A silica column used in hydrophobic interaction liquid chromatography (HILIC) mode was capable of differentiating GC and GalCer. The analysis of mouse brain samples revealed that GC accounted for only 0.3% of the total monohexosylceramides. Cer and LacCer were also profiled and quantified in mouse brain, lung, liver and spleen. Application of these methods greatly facilitated a range of targeted sphingolipidomic investigations and will permit a better understanding of the function and mechanism of these diverse molecular species in various disease animal models, including Gaucher disease.

Keywords: Sphingolipids; Mass spectrometry; Liquid chromatography; Galactosylceramides

Introduction

Sphingolipids (SLs) and glycosphingolipids (GSLs) are essential structural components of mammalian cell membranes. These lipid classes are critical for maintaining the structural integrity of the cell membrane, and play important roles in recognition and signaling pathways [1,2]. Disturbances in SL and GSL metabolism/degradation are associated with many lipid-storage diseases, but also are evident in other pathophysiological conditions, including neurological [3,4], skin [5,6], and lung [7] diseases, and in diabetes [8] and cancer [9,10]. There is now an increasing interest in qualitatively and quantitatively profiling different species of bioactive sphingolipids and related lipid classes; and this has now become possible with the advent of increasingly sensitive tandem mass spectrometry instrumentation.

Application of liquid chromatography coupled with electrospray ionization tandem mass spectrometry (LC-ESI-MS/MS) permits the in-depth profiling and quantification of sphingolipids with high sensitivity and specificity. By manipulation of the HPLC conditions, types of columns and solvent systems, and coupling to a triple-quadrupole mass spectrometer, individual lipids can be detected and quantified at the picomolar level, facilitating examination of their distribution in different tissues. Several LC-MS/MS methods have been used to measure sphingolipids from sphingoid bases and their 1-phosphate [8,11-15] to ceramides [13,15-19], sphingomyelins [15,20-25], simple mono- and dihexosylceramides [15,22,26], and more complex glycosphingolipids. Several methods [12,13,15] permit a global analysis of sphingolipid species ranging from very polar species, i.e., sphingosine-1-phosphate, to more lipophilic species in the sphingolipid biosynthesis pathway. In many of these methods, sphingolipids with varying chain lengths often coelute under the chromatographic conditions used, thus making differentiation of closely related species reliant upon measurement of their specific masses. This approach can be problematic because of the natural isotopic contributions, which cause interferences between the ion channels being monitored for compounds of similar mass.

Here we report an LC-MS/MS method for profiling individual sphingolipids with adequate chromatographic resolution to overcome such potential isotopic effects. This highly specific and sensitive LC-MS/MS analytical approach affords the characterization of sphingolipids that vary in N-acyl chain lengths. Furthermore, the liquid chromatography mobile phase was optimized for the separation of individual glucosylceramide (GC), glucosylsphingosine (GS), ceramide (Cer), lactosylceramide (LacCer) and sulfatide species that vary in N-acyl chain lengths. We provide evidence of the applicability of this methodology to the analysis of these classes of lipids in tissue samples. The potential of this methodology is illustrated from the ability to map and compare quantitatively changes in sphingolipid distribution from wild type mice with that of a genetic mouse model of the lysosomal storage disease, Gaucher disease [27,28].

Materials and Methods

Reagents

Synthetic sphingolipid standards including glucosylsphingosine, N-acyl glucosylceramide (C8, C12, C16, C18, C24-1 GC), N-acyl galactosylceramide (C12, C16, C24-1 GalCer), N-acyl ceramide (C16, C17, C18, C24 Cer) and N-acyl lactosylceramide (C12, C16, C24 LacCer) in 99% purity were from Avanti Lipids, Inc (Alabaster, AL). Semisynthetic N-acyl sulfatide (C12, C16, C24 sulfatide) were from Matreya, Inc. (Pleasant Gap, PA). All other solvents and chemicals in either high performance liquid chromatography (HPLC) grade or

*Corresponding author: Kenneth Setchell, Cincinnati Children's Medical Center The Department of Pathology and Laboratory Medicine, 3333 Burnet Avenue, MLC 7019, Cincinnati, Ohio, USA, Tel: (513) 636-4548; Fax: (513) 636-7853; E-mail: kenneth.setchell@cchmc.org

analytical purity were from Sigma-Aldrich (St. Louis, MO). The strain background of WT mice was FVB and 9V/null (D409V/null) was mix of FVB, C57BL/6J and129SvEVBrd. The mice were maintained in micro isolators in accordance with institutional guidelines under IACUC approval at Cincinnati Children's Research Foundation.

Extraction of sphingolipid from mouse tissues

Tissue samples (~100 mg wet weight) were homogenized for 15 sec (PowerGen 35, Fisher Scientific) in a mixture of water (0.6 mL) and methanol: chloroform (2:1, v/v, 3 mL). The homogenates were shaken for 15 min and centrifuged for 5 min at 1,000 g. The pellets were then re extracted with water (0.7 mL) and methanol: chloroform (2:1, v/v, 3 mL). The combined extracts were centrifuged (5 min at 7,000 g). The supernatants were transferred to glass tubes and the solvents evaporated under a stream of nitrogen gas. The dried extracts were subjected to KOH alkaline methanolysis (0.3 N, 0.6 mL) to remove potentially interfering glycerolipids and incubated at 37°C for 1 h. After cooling, approximately 50 μL of 3N HCl was added. Then, water (50 μL) and chloroform (1.2 mL) were added to the solutionprior to loading the sample on a fine Sephadex G-25 column to remove non-lipid contaminants. The Sephadex G-25 column was prepared in chloroform: methanol: water (60/30/4.5, v/v/v). Sphingolipid species were collected in 10 mL of the above solvent and the sample was driedunder nitrogen gas.

Preparation of standards and samples for LC-MS/MS analysis

Stock solutions of sphingolipid standards (1 mg/mL) were prepared in chloroform: methanol (1:4, v/v) and stored at -20°C. Working solutions were prepared by dilution of the stock solutions with methanol. Calibration curves were constructed for C16, C18 and C24:1 GCs using C12GC as the internal standard. Quantification of GCs with various chain lengths was accomplished using the curve for the GC of closest chain length. The quantification of GS was based on the calibration curve using C8 GC as internal standard. For Cer analysis, C16, C18 and C24 Cers were used and C17 Cer was employed as the internal standard. C16 and C24 sulfatide standards were used to construct calibration curves and C12 sulfatide was used as an internal standard. In the method for GC/GalCer analysis, 5 standards (C16, C18, C24:1 GC and C16, C24:1 GalCer) were used and C12 GC and C12 GalCer were used separately as internal standards. The biological extracts, after clean up, were dissolved in methanol and spiked with the internal standards. Samples (10 μL) were injected on-column for LC/MS/MS analysis. Depending on the organ and genotype, different amounts of tissues (1-5 mg) were subjected to the analysis to allow the quantification within the dynamic range of the calibration curves.

Sphingolipid analyses by LC-MS/MS

Analysis was carried out by LC-ESI-MS/MS using a Waters Quattro Micro API triple quadrupole mass spectrometer (Milford, MA) interfaced with Acquity UPLC system. Nitrogen was the nebulizer gas and argon was the collision gas. The source temperature was maintained at 120°C, and the desolvation temperature was maintained at 425°C. The drying gas (N_2) was maintained at ca. 800 L/h, and the cone flow gas was turned off. The multiplier was set at an absolute value of 650 V. Optimized parameters, i.e., cone voltage and collision energy for GC, GS, Cer, Sulfatide and GalCer were determined by prior infusion of the individual compounds. For quantification of GC, Cer and LacCer, the ESI-MS/MS was operated in the multiple reaction monitoring (MRM) mode, with detection of the transition pair of the individual protonated parent ions and their common daughter ion m/z 264.GS was measured by monitoring of the

mass transition m/z 462.3>282.4. Sulfatides were analyzed in negative ion mode by detection of their parent ion and common daughter ion of m/z 97.

Online chromatographic separation for GC, GS, Cer, LacCer and Sulfatide was achieved using a Supelcosil-LC-18-DB column (33×3.0 mm i.d.3.0 μm). Gradient elution with a mobile phase of methanol and water charged with ammonium formate and formic acid was employed. The gradient started with 50% mobile phase A (water with 2 mM ammonium formate and 0.1% formic acid) for 1.1 min, followed by linearly over 1.2 min with 80% mobile phase B (methanol with 2 mM ammonium formate and 0.1% formic acid), and finally changed to 100% mobile phase B over an 8 min period, and held isocratic for 5 min. The gradient was then returned to 50% mobile phase A in 0.1 min and held for a further 2.9 min to equilibrate the LC column. The total analysis time was 15 min. This mobile phase gradient yielded excellent separation of sphingolipid subspecies of varying acyl chain length.

The chromatographic resolution of GC and GalCer was achieved by modification of a method published previously (15). A silica column (Supelco 2.1*250 mm) run in HILIC (hydrophobic interaction liquid chromatography) mode, using an isocratic mobile phase (0.6 mL/min) of acetonitrile/methanol/acetic acid, (97/2/1, v/v/v, with 5 mM ammonium acetate) was found to adequately resolve these two isomers with an analysis time of 8 min.

Results

HPLC-MS/MS for sphingolipid analyses

Sphingolipids are highly diverse in structure with large numbers of possible combinations of hydrophobic backbone and head groups (Figure 1). For example, Cers occur with or without a double bond in the backbone (ceramide vs dihydroceramide), or with a hydroxyl group at the α, or α and β positions forming α-OH ceramide and phytoceramide. The N-acyl chain length can vary from 14 to 36 carbons, with and without a double bond, thus giving large number of possible subspecies under a single category of compound. Given the complexity of these molecules and their closely related molecular weights, it was essential to optimize the LC conditions to chromatographically resolve the different subspecies in order to minimize possible interferences from natural isotope contributions of species with similar mass that otherwise may chromatographically overlap. To this end, ultra performance liquid chromatography (UPLC) columns were used since they have smaller particle sizes than conventional HPLC columns and facilitate superior chromatographic resolution. Indeed, this approach significantly improved the resolution patterns of sphingolipids. Our initial studies with a Waters Acquity UPLC column (BEH C18-1.7 μm, 50×2.1 mm i.d.) yielded excellent separation of glucosylceramide standards based upon their N-acyl chain length. Since this column could accommodate a relatively high flow rate (0.5 mL/min), SL species, including GS, GC, Cer, LacCer and sulfatide, were all eluted within a 15 min analytical run time with subspecies of different N-acyl chain lengths well resolved and with excellent peak shape (data not shown). Despite this advantage, the performance of this UPLC column was found to deteriorate significantly after it was exposed to relatively small numbers of mouse tissue sample extracts - the peak shape deteriorated, significant tailing was observed. The column could not be regenerated due to matrix contamination. Due to these limitations, a Supelco C18 column with larger diameter and shorter length (33×3.0 mm i.d.3.0 μm) was used at a high flow to maintain a rapid analysis time. This column and method proved robust enough to run about 2000 biological samples on the
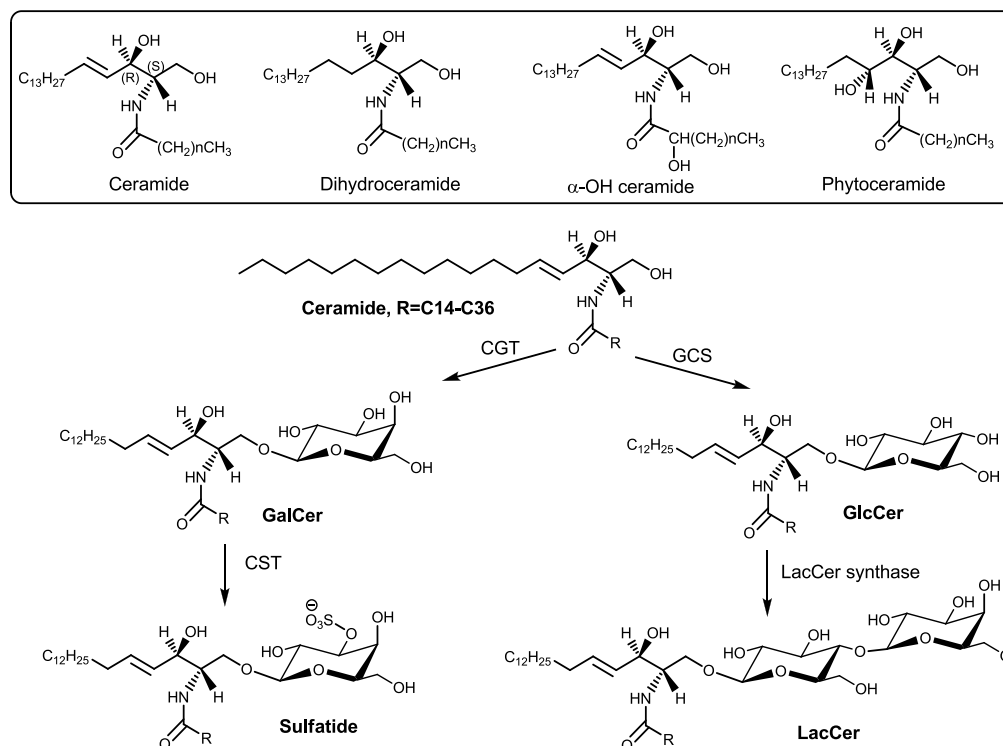
Figure 1: Biosynthetic pathway of GlcCer, LacCer, Galcer and Sulfatide from ceramide. Enzymes involved in the biosynthesis are glucosylceramide synthase (GCS), LacCer synthase, ceramide UDP-galactosyltransferase (CGT) and GST.

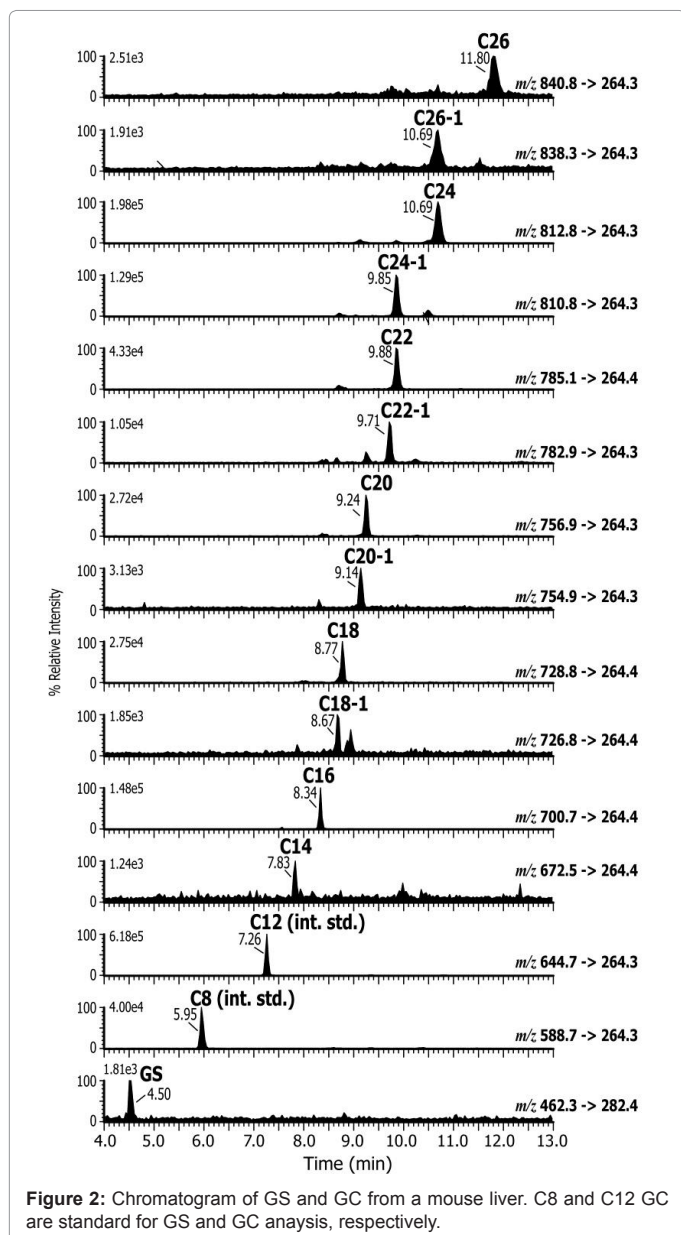|	SL	MRM transition ion pair (m/z)	Calibration curve	Correlation coefficient (r2)	LOD (S/N=5)
Cer	C16	538.6>264.3	y=0.4746x-0.0068	0.9911	1 pg
	C18	566.6>264.3	y=0.5681x-0.0117	0.9905	1 pg
	C24	650.7>264.3	y=0.3270x-0.0040	0.9917	1 pg
GC	C16	700.7>264.4	y=0.1856x-0.0016	0.9950	1 pg
	C18	728.8>264.4	y=0.2757x-0.0016	0.9982	1 pg
	C24-1	810.8>264.3	y=0.3202x-0.0029	0.9941	1 pg
LacCer	C16	862.7>264.3	y=1.7887x+0.0055	0.9986	1 pg
	C24	974.8>264.3	y=1.3099x+0.0027	0.9991	10 pg
Sulfatide	C16	778.7>97.0	y=0.1252x+0.0100	0.9942	50 pg
	C24	890.6>97.0	y=0.4184x+0.0361	0.9917	50 pg
Curves for GC and GalCer on SP-LC-MS/MS					
GC	C16	700.7>264.4	y=0.2163x-0.0013	0.9997	25 pg
	C18	728.8>264.4	y=0.2370x+0.0007	0.9999	25 pg
	C24-1	810.8>264.3	y=0.2243x-0.0018	0.9997	25 pg
GalCer	C16	700.7>264.4	y=0.2275x-0.0071	0.9997	25 pg
	C24-1	810.8>264.3	y=0.3142x-0.0083	0.9996	25 pg

Table 1: Calibration curve parameters for sphingolipid species.

same column and was consequently adopted for routine analysis.

The reverse phase LC-MS method described was able to differentiate SL species with differing N-acyl chain lengths. A typical mass chromatogram showing separation of GCs and GS in an extract of mouse liver (Figure 2) illustrates the separation of these subspecies. The predominant GC in mouse liver, C24:1 GC was well resolved from C24 GC and therefore the M+2 isotope of C24:1 GC did not interfere with the measurement of C24 GC. Calibration curves for GC, GS, Cer and Sulfatide were linear and reproducible over the dynamic range of 0.05 -25 ng (Table 1). The MRM transition pairs that were monitored to detect the individual sphingolipids, the calibration statistics and limit of detection (LOD) of the assays are summarized in Table 1. The

majority of the sphingolipids were readily detected at a signal/noise ratio of 5:1 down to a level of 1 pg injected on-column. Three liver extracts were tested for assay reproducibility for GC. Within- batch and between-batch variations were between 2.7-8.2% and 5.1-10.7%, respectively in the concentration range of 1.9-32.8 pmol/mg tissue.

A silica column operated under hydrophobic interaction liquid chromatography (HILIC) mode was found to resolve GC and GalCer, which is essential for analyses of brain tissue extracts, because of the abundance of galactosylceramide. However, the method gave partial or no separation of subspecies differing in chain length. Thus, cross-contamination from naturally occurring M+2 isotope contributions need to be taken into account when quantifying levels because of the

Figure 2: Chromatogram of GS and GC from a mouse liver. C8 and C12 GC are standard for GS and GC anaysis, respectively.

high mass of these compounds. The theoretical isotopic contributions calculated from software programs, e.g. Chemdraw (Cambridge, MA) are not always helpful for the determination of interfering natural isotopic contributions because many of the LC-MS/MS methods use multiple reaction monitoring function. For example, C24:1 GC has a theoretical value of 15% for its M+2 isotopic contribution. However, when C24:1 GC and GalCer standards at two different concentrations (10 ng/µL and 1 ng/µL, with 100 ng and 10 ng, respectively injected on column) were used to experimentally determine the M+2 isotopic contributions for the MRM transitions, the observed mean (± SD, n=6) values were 8.40 ± 0.05% and 8.18 ± 0.18%, respectively. The numbers were much lower than the theoretically calculated value and lower than the experimental value for the parent ion when it was analyzed by SIR (14.24 ± 0.39%). This difference is explained by the fact that isotopes of the daughter ions (m/z 264) for these hexosylceramides are not acquired under the specific MRM conditions and consequently the isotopic contributions for the M+2 ions will be lower than the theoretical values. Ultimately, rather than correcting for natural

isotopic interferences between ion channels, the best way to improve accuracy in quantification of these closely related sphingolipid species is to optimize the chromatographic conditions to attain complete chromatographic separation.

Application of LC-MS/MS to the analyses of mouse tissue sphingolipids

Ceramide is formed by the condensation of serine and palmitoyl CoA on the cytoplasmic face of endoplasmic reticulum (ER) and is the core compound for the biosynthesis of more complex sphingolipids, including glucosylceramide, lactosylceramide, galatosylceramide and sulfatide (Figure 1). There is considerable interest in quantifying levels of these complex lipids in physiologic and pathophysiologic states [29-31]. The current methods we developed were used to characterize and quantify these lipid classes in a variety of mouse spleen, liver, lung, and brain. A map of the composition and distribution of these lipid classes can provide a basis for evaluating pathophysiological changes in disease. Mice tissues (wild type, 9 weeks) were harvested, extracted following the methodology described and analyzed by LC-MS/MS for GC, Cer, LacCer and GalCer species. Of 18 different ceramide and α-hydroxyl ceramide subspecies that were monitored, the C16, C18, C20, C24-1 and C24 were the major species identified in wild-type mouse brain, lung, liver and spleen (Figure 3). N-stearoyl (C18) ceramide was the predominant ceramide in mouse brain, accounting

Figure 3: Chromatogram of ceramide subspecies from a mouse kidney.
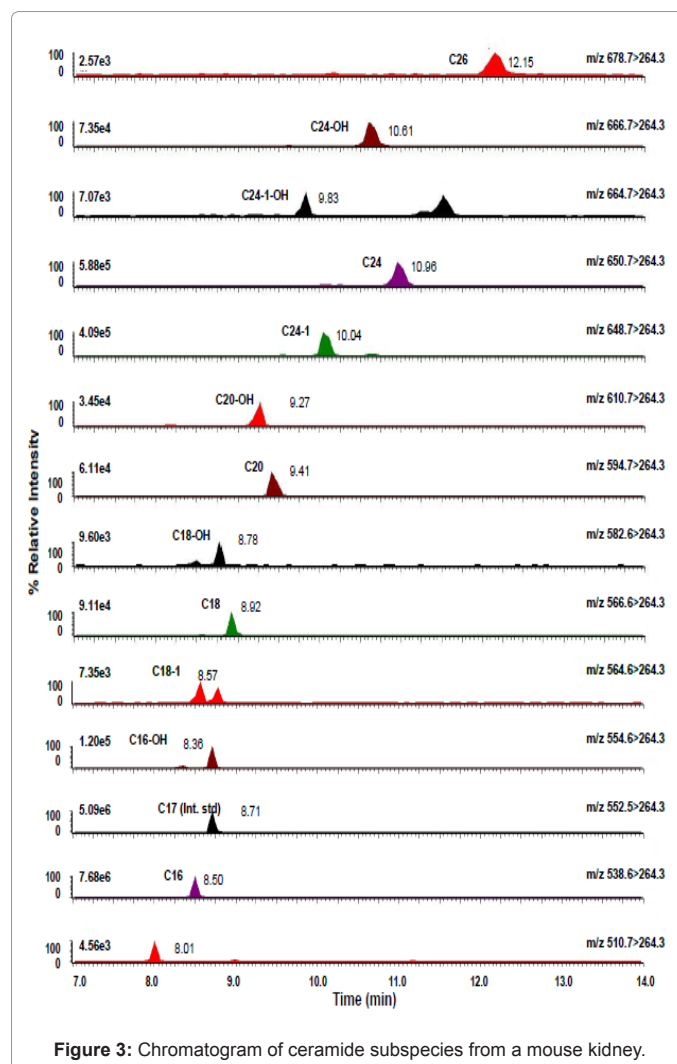
for 82% of the total ceramides identified, but in lung and spleen, it accounted for only 7% of the total, while in liver it was present in low abundance (3%). The characteristic high level of sphingolipids with N-stearoyl acid in brain is associated with a high expression level of the stearoyl-CoA specific ceramide synthase [32]. Total ceramide levels in lung, liver and spleen were similar with average values of 140-180 pmol per mg tissue (Table 2). In brain, the average total Cer level was about 110 pmol/mg tissues, which was 20-40% lower than in visceral tissues. The ceramide subspecies had similar distribution patterns and concentrations in visceral tissues, but was considerably different in the brain. C24-1 Cer was the predominant species in mouse lung, liver and spleen (56-68 pmol/mg tissue) while in brain it was found at a much reduced level of only 11 pmol/mg tissue. Likewise, the C24 Cer level ranged 30-51 pmol/mg in mouse visceral tissues and only 2.3 pmol/mg in brain. A detailed list of the tissue levels of these ceramides are shown in Table 2.
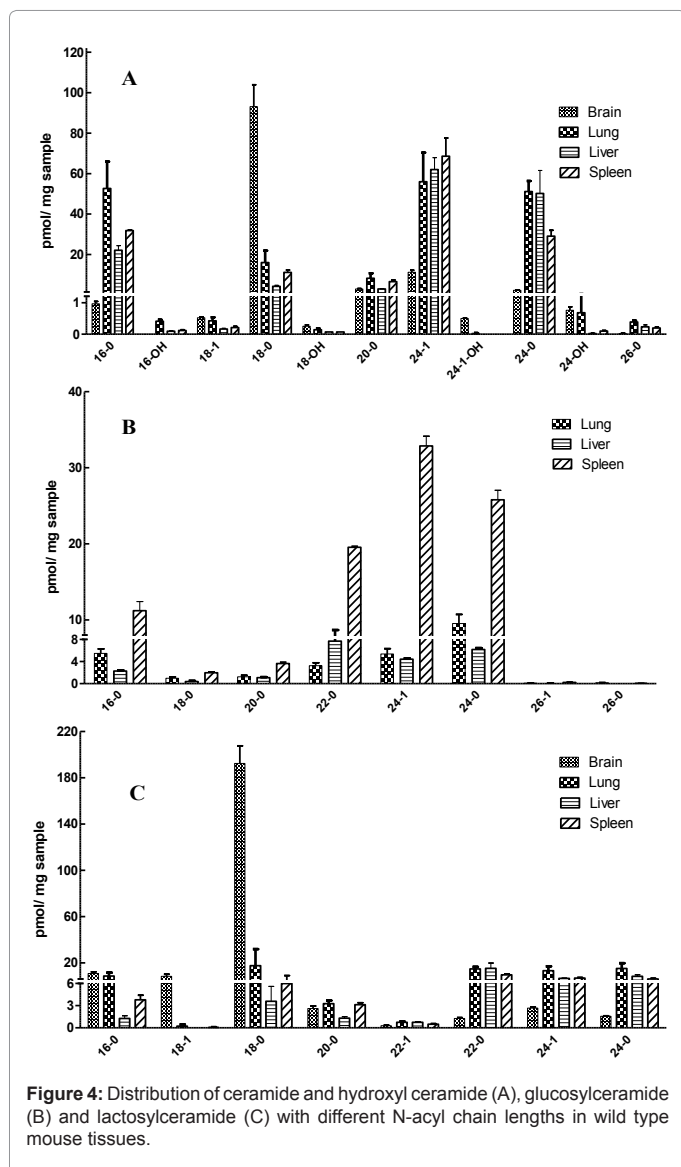
The qualitative and quantitative distribution of GC in wild-type mouse spleen, liver, and lung are shown in Figure 4. The major GCs contained C24-1, C24, C22, C16, C20, and C18 fatty acid acyl chains; GCs with other chain lengths, if present, were below the limit of detection of the method (0.02 pmol/mg tissue). The average total GC levels in spleen, liver and lung from 3 wild-type mice were 95.3, 26.1, 22.1 pmol/mg tissue, respectively. The GC concentrations in spleen were consistently 3-5 times higher than those in liver and lung (Figure 4). The C24-1 GC was the most predominant GC in spleen and was 7 times higher than in the liver and lung. Overall, C24-1, C24, C22, C16 GCs collectively comprised 90% of the total GCs detected in these tissues, although there was some variation in the distribution patterns among different tissues (Figure 5). For example, C24-1 GC was the predominant glucosylceramide in mouse spleen, whereas C22 GC was the predominant species in the liver and C24 GC the predominant species in the lung.

When Johan L. W. Thudichum discovered glycosphingolipids from brain in 1884 [33], the sugar moiety was defined as D-galactose, an isomer of D-glucose. Indeed, galactosylceramides are the predominant monohexosylceramide species present in brain. Using a silica column for hydrophobic interaction liquid chromatography (HILIC), GC and GalCer were selectively detected and quantified. Of four wild type mouse brain samples analyzed, total monohexosylceramide levels were in the range of 1037-1651 pmol/mg tissue; GC accounted for 0.3% of the total monohexosylceramides and C18, C24-1, C24 GC were major species detected. Eleven different GalCers were found in mouse

Ceramide (pmol/mg sample)

subspecies	16-0	16-OH	18-1	18-0	18-OH	20-0	22-1	22-0	24-1	24-1-OH	24-0	24-OH	26-1	26-0	TOTAL
brain(n=3)	0.97± 0.07	0 ± 0	0.52 ± 0.02	93.09 ± 10.8	0.25 ± 0.05	2.99 ± 0.23			11.27 ± 0.98	0.5 ± 0.02	2.34 ± 0.18	0.76 ± 0.11		0.02 ± 0.02	112.71 ± 11.38
lung (n=3)	52.67 ± 13.23	0.41 ± 0.05	0.43 ± 0.11	16.05 ± 5.88	0.14 ± 0.04	8.31 ± 2.47			55.98 ± 14.34	0.02 ± 0.02	51.15 ± 5.22	0.68 ± 0.56		0.39 ± 0.04	186.22 ± 36.04
liver (n=3)	22.14 ± 2.23	0.1 ± 0.02	0.17 ± 0.02	4.26 ± 0.51	0.07 ± 0	3.01 ± 0.04			62.01 ± 5.89	0 ± 0	50.21 ± 11.37	0.02 ± 0.02		0.24 ± 0.06	142.21 ± 5.48
spleen (n=3)	31.83 ± 0.37	0.12 ± 0.02	0.21 ± 0.04	11.19 ± 1.11	0.07 ± 0	6.62 ± 0.79			68.61 ± 9	0 ± 0	29.12 ± 2.83	0.1 ± 0.02		0.2 ± 0.02	148.08 ± 14.01

Glucosylceramide (pmol/mg sample)

subspecies	16-0		18-1	18-0		20-0	22-1	22-0	24-1		24-0		26-1	26-0	TOTAL
lung (n=3)	2.29 ± 0.14			0.37 ± 0.15		1.09 ± 0.09		7.7 ± 0.97	4.43 ± 0.14		6.19 ± 0.26		0.02 ± 0.02	0 ± 0	22.08 ± 1.21
liver (n=3)	5.47 ± 0.82			0.99 ± 0.24		1.23 ± 0.26		3.26 ± 0.52	5.36 ± 0.98		9.52 ± 1.19		0.08 ± 0.02	0.16 ± 0.04	26.08 ± 3.97
spleen (n=3)	11.22 ± 1.19			1.98 ± 0.2		3.65 ± 0.26		19.55 ± 0.15	32.86 ± 1.29		25.79 ± 1.25		0.22 ± 0.06	0.06 ± 0.02	95.34 ± 1.77

Lactosylceramide (pmol/mg sample)

subspecies	16-0		18-1	18-0		20-0	22-1	22-0	24-1		24-0		26-1	26-0	TOTAL
brain(n=3)	0.83 ± 1.41		8.41±1.79	192.41±15.27		2.61±0.33	0.28 ± 0.07	1.27 ± 0.12	2.67 ± 0.12		1.57 ± 0.07				220.06 ± 18.47
lung (n=2)	8.58 ± 3.02		0.23±0.23	17.53 ± 14.38		3.27±0.44	0.74 ± 0.11	14.69 ± 1.8	13.27 ± 3.81		15.09 ± 4.62				73.4 ± 0.83
liver (n=2)	1.28 ± 0.35		0 ± 0	3.6 ± 2.02		1.31 ± 0.22	0.74 ± 0.11	15.33 ± 4.54	6.58 ± 0.21		8.42 ± 1.23				37.25 ± 7.13
spleen (n=3)	3.79 ± 0.62		0.08 ± 0.08	5.99 ± 3.07		3.12 ± 0.26	0.49 ± 0.07	9.58 ± 0.67	6.86 ± 0.45		6.02 ± 0.6				35.94 ± 2.09

Galactosylceramide (pmol/mg sample)

subspecies	16-0	18-1	18-0	20-1	20-0	22-1	22-0	24-1	24-0	26-1	26-0	TOTAL
brain (n=3)	3.96 ± 0.66	2.47 ± 0.56	29.03 ± 17.15	1.86 ± 0.45	21.23 ± 2.49	33.66 ± 4.84	33.68 ± 4.74	941.66 ± 95.77	143.91 ± 19.16	11.26 ± 1.12	3.22 ± 0.53	1325.94 ± 141.61

Sulfatide (pmol/mg sample)

subspecies	16-0	18-1	18-0	20-1	20-0	22-1	22-0	24-1	24-0		TOTAL
brain (n=3)	3.34 ± 0.53	12.21 ± 2.42	126.63 ± 8.59	1.48 ± 0.14	13.88 ± 1.5	7.78 ± 0.75	7.76 ± 0.74	96.82 ± 6.11	48.71 ± 3.78		460.37 ± 24.85
	16-OH	**18-1-OH**	**18-OH**	**20-1-OH**	**20-OH**	**22-1-OH**	**22-OH**	**24-1-OH**	**24-OH**		
	0 ± 0	1.3 ± 0.2	38 ± 1.54	0.98 ± 0.12	4.4 ± 0.59	2.28 ± 0.11	33.88 ± 0.2	22.31 ± 0.38	28.61 ± 0.14		

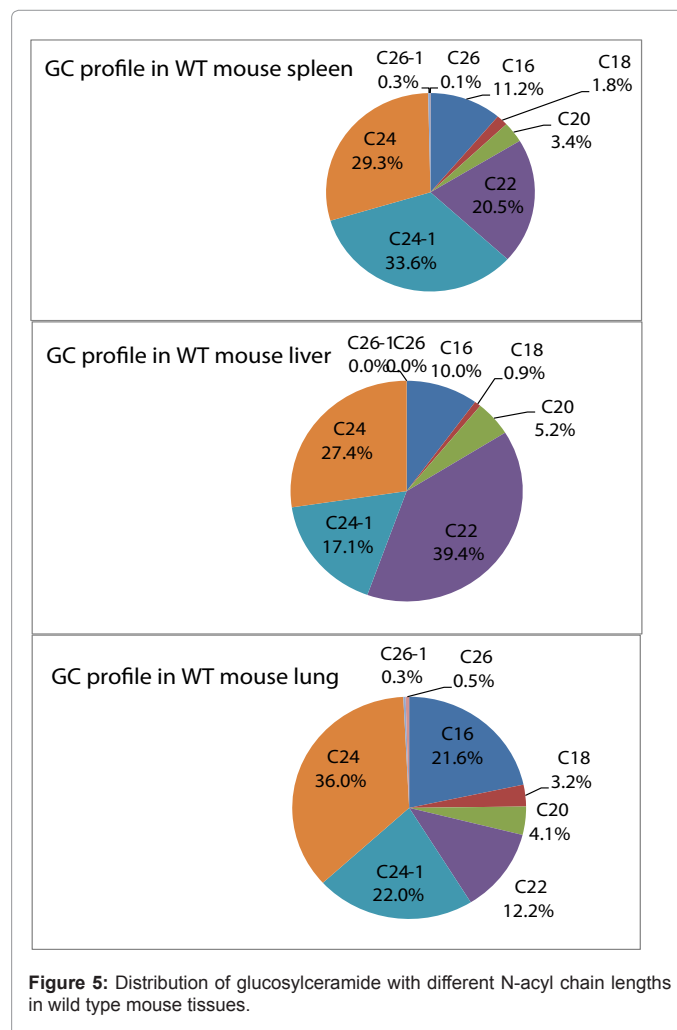**Table 2:** Profile of sphingolipids in wild type mouse tissues.

Figure 4: Distribution of ceramide and hydroxyl ceramide (A), glucosylceramide (B) and lactosylceramide (C) with different N-acyl chain lengths in wild type mouse tissues.

Sulfatide is a 3-sulfated derivative of galactosylceramide. Sulfatide is present in high concentrations in the nervous systems, particularly in the myelin sheath of brain and in peripheral nerves [34]. Sulfatide fulfills important functions in oligodendrocyte differentiation, formation of the paranodal junctions, and myelin maintenance [35,36]. Accumulation of sulfatide has been reported in several human diseases, particularly metachromatic leukodystrophy [37] and Alzheimer's disease [38]. Elevated sulfatide levels in neurons causes lethal audiogenic seizures in mice [34]. Previous analyses of mouse brain suggested that the major sulfatide species are C18, C20, C22, C24-1 and C24 sulfatide [39]. Since liquid chromatography can be used to concentrate sulfatide compounds on the column before detection by mass spectrometry, 17 different sulfatide and hydroxyl sulfatide species were detected (Figure 6) and quantified (Table 2). The major sulfatid species identified in brain were C18, C24-1, C24-sulfatides and C18, C22, C24-1, C24 hydroxyl sulfatides, which accounted for 86% of the total sulfatide present.

Accumulation of glucosylceramide and glycosylsphingosine in Gaucher disease mouse model

These methods were applied to a mouse model of Gaucher disease in which GC and GS accumulate [40]. The mouse had a point mutated *Gba1* allele, D409V, and a null allele to give the genotype of D409V/null. Visceral tissues from these mice have acid β-glucosidase activities at 4.0-6.8% of wild-type [40]. Using TLC, varying degrees
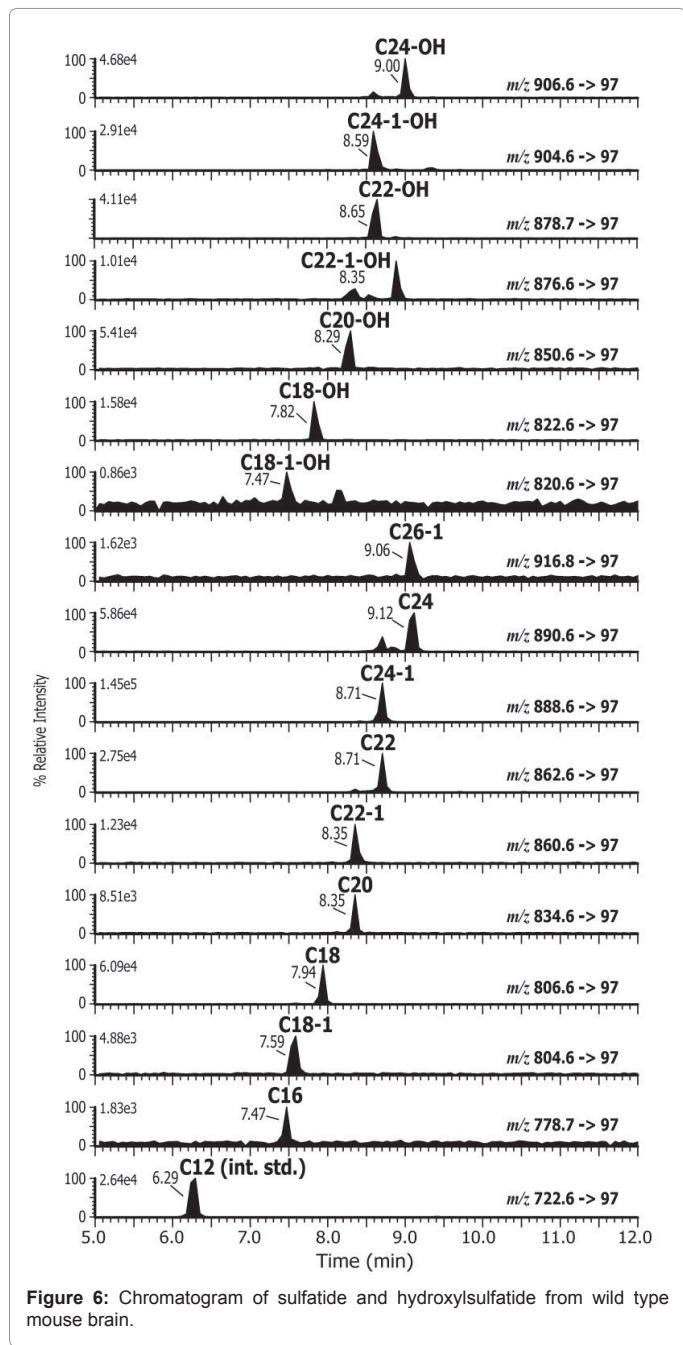
brain. These were C16, C18-1, C18, C20-1, C20, C22-1, C22, C24-1, C24, C26-1 and C26 GalCer. Of these, C24-1 GalCer comprised about 70% of the total GalCer, while C24 and C18 GalCer each accounted for about 10% of the total GalCer pool. The C20, C22-1, C22 GalCer species contributed only 1.5-3.0% to the total GalCer pool (Table 2).

After ceramide is converted to glucosylceramide, further stepwise addition of sugars give rise to a wide variety of complex glycosphingolipids, e.g. lactosylceramide. The present methods were expanded to the quantification of LacCer in different mouse tissues by selecting specific MRM transitions for these lipid species. The patterns of LacCer in brain, lung, liver and spleen were found similar to those of ceramide (Figure 4). In brain, C18 LacCer was again the most predominant species, accounting for 87% of the total LacCer. The C22, C24-1 and C24 LacCer were the major species in lung, liver and spleen and the levels ranged 6.0-15.3 pmol/mg tissue. By contrast, in brain, these species were at much lower concentrations (1.3-2.7 pmol/mg tissue). The individual lactosylceramides measured in the different tissues are in Table 2.

Figure 5: Distribution of glucosylceramide with different N-acyl chain lengths in wild type mouse tissues.

Figure 6: Chromatogram of sulfatide and hydroxylsulfatide from wild type mouse brain.

of GC accumulation were present in visceral organs of the D409V/null mice. However, the TLC method allows only assessment of total GC, but not compositional changes in individual GC species. The LC-MS/MS method was therefore applied to characterize the GC and GS levels in spleen, liver and lung tissues of wild-type and D409V/null mice (52-week old) (Figure 7). When the major GC species were compared between wild-type and the D409V/null mice (Table 3), the lung exhibited the highest level of accumulation, as displayed by a 22-65 fold increase over the wild-type mouse. By comparison, accumulations of these species in liver and spleen were at lower levels (7-31 fold change). In addition to differences in the quantitative levels of these lipids, the relative distribution of the different subspecies varied considerably among the wild-type and D409V/null mice and also within the different tissues. The C24 GC showed the highest

accumulation in lung compared to the C16, C22 and C24-1GC species, while in liver; the increase of C16 GC is most significant. These data confirmed a preferential accumulation of specific glucosylceramides in different tissues in this animal model.

Conclusion

In summary, the methods developed in this study allow for the mapping of a vast number of different sphingolipid classes at the tissue level and represents a powerful approach for future investigation of pathophysiological states where lipid accumulation may be important in the etiology of the condition. Furthermore, this approach may be helpful in evaluating the effectiveness of potential therapies for correcting some of the lipid dysfunction associated with diseases such as Gaucher disease.
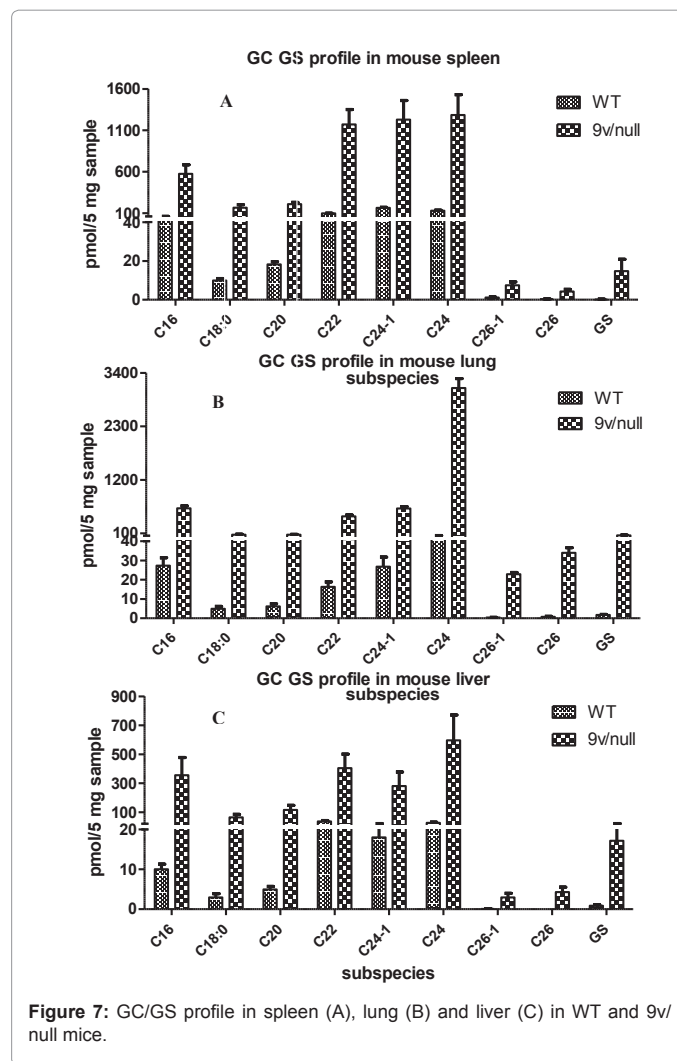
References

Figure 7: GC/GS profile in spleen (A), lung (B) and liver (C) in WT and 9v/null mice.

GC N-acyl ch ain length				
Tissue	**C16**	**C22**	**C24-1**	**C24**
Lung	22.5	27.6	22.8	64.9
Liver	31.1	10.5	12.7	19.3
Spleen	10.2	12	7.5	10

Table 3: Fold change of glucosylceramide species in Gaucher disease mouse model.

1. Lahiri S, Futerman AH (2007) The metabolism and function of sphingolipids and glycosphingolipids. Cell Mol Life Sci 64: 2270-2284.

2. Kolter T, Sandhoff K (2005) Principles of lysosomal membrane digestion: stimulation of sphingolipid degradation by sphingolipid activator proteins and anionic lysosomal lipids. Annu Rev Cell Dev Biol 21: 81-103.

3. Goker-Alpan O, Lopez G, Vithayathil J, Davis J, Hallett M, et al. (2008) The spectrum of parkinsonian manifestations associated with glucocerebrosidase mutations. Arch Neurol 65: 1353-1357.

4. Marks N, Berg MJ, Saito M (2008) Glucosylceramide synthase decrease in frontal cortex of Alzheimer brain correlates with abnormal increase in endogenous ceramides: consequences to morphology and viability on enzyme suppression in cultured primary neurons. Brain Res 1191: 136-147.

5. Hara J, Higuchi K, Okamoto R, Kawashima M, Imokawa G (2000) High-expression of sphingomyelin deacylase is an important determinant of ceramide deficiency leading to barrier disruption in atopic dermatitis. J Invest Dermatol 115: 406-413.

6. Ishibashi M, Arikawa J, Okamoto R, Kawashima M, Takagi Y, et al. (2003) Abnormal expression of the novel epidermal enzyme, glucosylceramide deacylase, and the accumulation of its enzymatic reaction product, glucosylsphingosine, in the skin of patients with atopic dermatitis. Lab Invest 83: 397-408.

7. Breslow DK, Collins SR, Bodenmiller B, Aebersold R, Simons K, et al. (2010) Orm family proteins mediate sphingolipid homeostasis. Nature 463: 1048-1053

8. Fox TE, Bewley MC, Unrath KA, Pedersen MM, Anderson RE, et al. (2011) Circulating sphingolipid biomarkers in models of type 1 diabetes. J Lipid Res 52: 509-517.

9. Ogretmen B, Hannun YA (2004) Biologically active sphingolipids in cancer pathogenesis and treatment. Nat Rev Cancer 4: 604-616.

10. Hakomori S (1996) Tumor malignancy defined by aberrant glycosylation and sphingo(glyco)lipid metabolism. Cancer Res 56: 5309-5318.

11. Mano N, Oda Y, Yamada K, Asakawa N, Katayama K (1997) Simultaneous quantitative determination method for sphingolipid metabolites by liquid chromatography/ionspray ionization tandem mass spectrometry. Anal Biochem 244: 291-300.

12. Sullards MC, Merrill AH Jr (2001) Analysis of sphingosine 1-phosphate, ceramides, and other bioactive sphingolipids by high-performance liquid chromatography-tandem mass spectrometry. Sci STKE.

13. Sullards MC (2000) Analysis of sphingomyelin, glucosylceramide, ceramide, sphingosine, and sphingosine 1-phosphate by tandem mass spectrometry. Methods Enzymol 312: 32-45.

14. Lieser B, Liebisch G, Drobnik W, Schmitz G (2003) Quantification of sphingosine and sphinganine from crude lipid extracts by HPLC electrospray ionization tandem mass spectrometry. J Lipid Res 44: 2209-2216.

15. Shaner RL, Allegood JC, Park H, Wang E, Kelly S, et al. (2009) Quantitative analysis of sphingolipids for lipidomics using triple quadrupole and quadrupole linear ion trap mass spectrometers. J Lipid Res 50: 1692-1707.

16. Bielawski J, Szulc ZM, Hannun YA, Bielawska A (2006) Simultaneous quantitative analysis of bioactive sphingolipids by high-performance liquid chromatography-tandem mass spectrometry. Methods 39: 82-91.

17. Liebisch G, Drobnik W, Reil M, Trumbach B, Arnecke R, et al. (1999) Quantitative measurement of different ceramide species from crude cellular extracts by electrospray ionization tandem mass spectrometry (ESI-MS/MS). J Lipid Res 40: 1539-1546.

18. Han X (2002) Characterization and direct quantitation of ceramide molecular species from lipid extracts of biological samples by electrospray ionization tandem mass spectrometry. Anal Biochem 302: 199-212.

19. Pettus BJ, Bielawska A, Kroesen BJ, Moeller PD, Szulc ZM, et al. (2003) Observation of different ceramide species from crude cellular extracts by normal-phase high-performance liquid chromatography coupled to atmospheric pressure chemical ionization mass spectrometry. Rapid Commun Mass Spectrom 17: 1203-1211.

20. Karlsson AA, Michelsen P, Odham G (1998) Molecular species of sphingomyelin: determination by high-performance liquid chromatography/ mass spectrometry with electrospray and high-performance liquid chromatography/tandem mass spectrometry with atmospheric pressure chemical ionization. J Mass Spectrom 33: 1192-1198.

21. Isaac G, Bylund D, Mansson JE, Markides KE, Bergquist J (2003) Analysis of phosphatidylcholine and sphingomyelin molecular species from brain extracts using capillary liquid chromatography electrospray ionization mass spectrometry. J Neurosci Methods 128: 111-119.

22. Merrill AH Jr, Sullards MC, Allegood JC, Kelly S, Wang E (2005) Sphingolipidomics: high-throughput, structure-specific, and quantitative analysis of sphingolipids by liquid chromatography tandem mass spectrometry. Methods 36: 207-224.

23. Shimizu A, Ashida Y, Fujiwara F (1991) Measurement of the ratio of lecithin to sphingomyelin in amniotic fluid by fast atom bombardment mass spectrometry. Clin Chem 37: 1370-1374.

24. Brugger B, Erben G, Sandhoff R, Wieland FT, Lehmann WD (1997) Quantitative analysis of biological membrane lipids at the low picomole level by nano-electrospray ionization tandem mass spectrometry. Proc Natl Acad Sci U S A 94: 2339-2344.

25. Pulfer M, Murphy RC (2003) Electrospray mass spectrometry of phospholipids. Mass Spectrom Rev 22: 332-364.

26. Suzuki M, Sekine M, Yamakawa T, Suzuki A (1989) High-performance liquid chromatography-mass spectrometry of glycosphingolipids: I. Structural 19 characterization of molecular species of GlcCer and IV3 beta Gal-Gb4Cer. J Biochem 105: 829-833.

27. Grabowski GA (2008) Phenotype, diagnosis, and treatment of Gaucher's disease. Lancet 372: 1263-1271.

28. Grabowski GA (2008) Treatment perspectives for the lysosomal storage diseases. Expert Opin Emerg Drugs 13: 197-211.

29. Koybasi S, Senkal CE, Sundararaj K, Spassieva S, Bielawski J, et al. (2004) Defects in cell growth regulation by C18:0-ceramide and longevity assurance gene 1 in human head and neck squamous cell carcinomas. J Biol Chem 279: 44311-44319.

30. Pewzner-Jung Y, Brenner O, Braun S, Laviad EL, Ben-Dor S, et al. (2010) A critical role for ceramide synthase 2 in liver homeostasis: II. insights into molecular changes leading to hepatopathy. J Biol Chem 285: 10911-10923.

31. Pewzner-Jung Y, Park H, Laviad EL, Silva LC, Lahiri S, et al. (2010) A critical role for ceramide synthase 2 in liver homeostasis: I. alterations in lipid metabolic pathways. J Biol Chem 285: 10902-10910.

32. Becker I, Wang-Eckhardt L, Yaghootfam A, Gieselmann V, Eckhardt M (2008) Differential expression of (dihydro)ceramide synthases in mouse brain: oligodendrocyte-specific expression of CerS2/Lass2. Histochem Cell Biol 129: 233-241.

33. Thudichum JLW (1884) A Treatise on the chemical constitution of the brain. Archon Books.

34. van Zyl R, Gieselmann V, Eckhardt M (2010) Elevated sulfatide levels in neurons cause lethal audiogenic seizures in mice. J Neurochem 112: 282-295.

35. Honke K, Tsuda M, Hirahara Y, Ishii A, Makita A, et al. (1997) Molecular cloning and expression of cDNA encoding human 3'- phosphoadenylylsulfate :galactosylceramide 3'-sulfotransferase. J Biol Chem 272: 4864-4868.

36. Eckhardt M (2008) The role and metabolism of sulfatide in the nervous system. Mol Neurobiol 37: 93-103.

37. Figureura K von, G, V, Jaeken J (2001) Metachromatic leukodystrophy. In The Metabolic and Molecular Bases of Inherited Disease, McGraw-Hill, New York 3695-3724.

38. Han X, M Holtzman D, McKeel DW Jr, Kelley J, Morris JC (2002) Substantial sulfatide deficiency and ceramide elevation in very early Alzheimer's disease: potential role in disease pathogenesis. J Neurochem 82: 809-818.

39. Asakawa D, Yoshimura K, Takeda S, Hiraoka K (2010) Direct analysis of lipids in mouse brain using electrospray droplet impact/SIMS. J Mass Spectrom 45: 437-443.

40. Xu YH, Quinn B, Witte D, and Grabowski GA (2003) Viable mouse models of acid beta-glucosidase deficiency: the defect in Gaucher disease. Am J Pathol 163: 2093-2101.